Ultrasonic bonding of flexible PCB to rigid PCB using an Sn interlayer

Kyoo-Seok Kim and Jae-Pil Jung
Department of Materials Science and Engineering, University of Seoul, Seoul, South Korea, and

Y. Norman Zhou
Department of Mechanical Engineering, University of Waterloo, Waterloo, Canada

Abstract

Purpose – The aim of the paper is to study the feasibility of direct ultrasonic bonding between contact pad arrays on flexible printed circuit boards (FPCB) and rigid printed circuit boards (RPCB) at ambient temperature.

Design/methodology/approach – Metallization layers on the RPCB comprised Sn on Cu while the pads on the FPCB consisted of Au/Ni/Cu. Prepared RPCB and FPCB were bonded by ultrasound at ambient temperature using an ultrasonic frequency of 20 kHz, a power of 1,400 W, and 0.62 MPa of bonding pressure. The bonded samples were cross-sectioned and the joints and microstructures were observed by Field Emission Scanning Electron Microscopy (FE-SEM) and Energy Dispersive Spectroscopy (EDS). The soundness of the joints was evaluated by pull testing.

Findings – Robust bonding between FPCB and RPCB was obtained by bonding for 1.0 and 1.5 s. This result has confirmed that direct room temperature ultrasonic bonding of Au and Sn is feasible. At a longer bonding time of 3.0 s, cracks and voids were found in the joints due to excessive ultrasonic energy. The IMC (intermetallic compound) between the Sn layer and pads of the RPCB was confirmed as Cu_6Sn_5. On the FPCB side, Cu_6Sn_5 and Ni_3Sn_4 were formed by contact with the facing Sn coating, and mechanically alloyed $Cu_{0.81}Ni_{0.19}$ was found within the pads. Meanwhile, the strength of bonded joints between FPCB and RPCB increased with bonding time up to 1.5 s and the maximum value reached 12.48 N. At 3.0 s bonding time, the strength decreased drastically, and showed 5.75 N. Footprints from the fracture surfaces showed that bonding started from the edges of the metal pads, and extended to the pad centers as ultrasonic bonding time was increased.

Originality/value – Direct ultrasonic bonding with transverse vibration at ambient temperature between the surface layers of the pads of FPCB and RPCB has been confirmed to be feasible.

Keywords Printed circuits, Joining processes, Bonding

Paper type Research paper

1. Introduction

Interconnection technology for joining metallic pads of flexible printed circuit boards (FPCB) to the outer leads of modules, displays, rigid printed circuit boards (RPCB) and similar components is of increasing importance in the electronics industry. The FPCB is light, thin and flexible to fit into compact electronic devices and it can be applicable to various electronic products such as liquid crystal display (LCD) modules, hand held electronics and so on. Currently, a widely used method for the interconnection of FPCB is adhesive bonding using an anisotropic conductive film (ACF). The ACF or anisotropic conductive adhesives (ACA) are useful for applications which require fine pitch bonding and thin packages such as chip-on-glass (COG), chip-on-film (COF), PCBs, LCD assembly and flip chip packaging (Fan *et al.*, 2003, Frisk *et al.*, 2006). However, the ACF is expensive and shows low electrical conductivity due to the mixture of conducting metal and non-conducting polymer resin (Fan *et al.*, 2003). The ACF also needs higher temperature of the order of 100-200°C and pressure in the range 1-100 MPa for bonding (Seppala *et al.*, 2003, Frisk *et al.*, 2006, Wu *et al.*, 2001).

Meanwhile, ultrasonic bonding has advantages of short bonding time, low bonding temperature and pressure, low cost and better electrical conductivity (Graff *et al.*, 2007) and these characteristics have resulted in very wide application of ultrasonic bonding to flip chips (Hong *et al.*, 2002), wire bonding (Chan *et al.*, 2006), and other packaging (Kim *et al.*, 2002, Shi *et al.*, 2000).

The ultrasonic bonding process is efficient for copper, but can be difficult for very soft metals like lead and tin, where these metals are used as electric contacts for electronic parts or pads on PCBs. As an example of previous study for the ultrasonic bonding of Sn-based metals, thermosonic bonding between Au bump and Sn-3.0 wt percent Ag-0.5 wt percent Cu was reported (Lee *et. al.*, 2005a). Ultrasonic bonding of RPCB and FPCB pads with longitudinal vibration at a heated state was carried out by the author *et al.* (Lee *et al.*, 2008). However, ultrasonic bonding with transverse vibration at

The current issue and full text archive of this journal is available at
www.emeraldinsight.com/0954-0911.htm

Soldering & Surface Mount Technology
21/1 (2009) 4–10

[DOI 10.1108/09540910910928256]

This study was carried out with the financial support of Seoul R&BD project of 2008.

Received: 4 March 2008
Revised: 5 October 2008
Accepted: 12 October 2008

ambient temperature between Sn and Au, the outer layers of the respective pads of the FPCB and RPCB in this work, or between Sn and Ni, the subsequent layers under Au, was not reported.

Thus, in this study the feasibility of direct ultrasonic bonding at ambient temperature between metal pads of FPCB and RPCB without ACF was investigated. The bonding was carried out between outer leads (metallic pads) of the respective PCBs. Bonding characteristics, microstructure and mechanical properties were investigated for these ultrasonically bonded joints.

2. Experimental

Representative RPCB and FPCB were used as bonding samples. The size of the RPCB was 20 × 18 mm with 1 mm thickness and the FPCB was 10 × 8 mm with 70 μm thickness. Each PCB of both types had a single row of ten metallized pads along one edge. The dimensions of the pads on both PCBs were 2.5 × 0.5 mm with a pad pitch of 0.9 mm. The metal pads on the RPCB consisted of Sn and Cu from top to bottom with thickness of 0.50 μm and 30 μm, respectively. The pads on the FPCB were composed of Au, Ni, and Cu from top to bottom, of thicknesses 0.03 μm, 0.3 μm and 10 μm, respectively. All of the pads were formed by electroplating and an additional Sn interlayer with a thickness of 50 μm was applied to the RPCB pads by dip-plating in a molten Sn-bath at 523 K for one second to secure good bondability with the FPCB.

For bonding, RPCB/FPCB pairs had their pad arrays aligned and then ultrasound was applied to bond all ten pad pairs simultaneously. Figure 1 shows a schematic diagram of the experimental apparatus used for ultrasonic bonding. Experimental conditions for ultrasonic bonding were 20 kHz ultrasonic frequency, 1,400 W of transducer power, and 0.62 MPa bonding pressure (0.009 N to each pad). The bonding time was varied from 0.3 to 3.0 s, and bonding was carried out at ambient temperature without heating the samples. The ultrasonic sonotrode tip vibrated horizontally, and thus the ultrasonic amplitude was applied parallel to the joint plane.

Figure 1 Schematic diagram of the ultrasonic (US) bonding setup for joining FPCB and RPCB (US frequency; 20 kHz, power; 1,400 W)

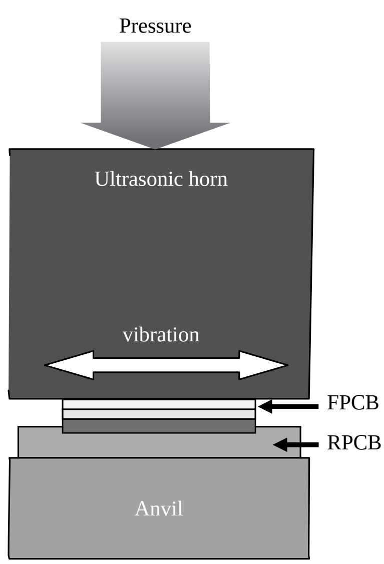

The bonded joints between the metal pads of the FPCB and RPCB were analysed by Scanning Electron Microscopy (SEM) and Energy Dispersive Spectroscopy (EDS). A Field Emission SEM (FE-SEM) was used for investigating microstructure and intermetallic compounds (IMC), with EDS for the analysis of chemical composition of the IMC. The IMC phases along the bonded interface were confirmed by X-ray diffractometer (XRD). For the XRD analysis, Sn in the bonded interface was etched away from the IMCs. Bond strength at the joint was evaluated by pull testing as shown in Figure 2. Pull speed was 200 μm/s, and the angle between the RPCB and FPCB was 45°. Five pull tests were performed for each ultrasonic bonding condition. The fractured surfaces of the bonded joints were then examined by SEM.

3. Results and discussion

3.1 Microstructure in the joints

Figure 3 shows representative cross sections of the ultrasonic bonded joints between FPCB and RPCB versus bonding time. In the sample of 0.3 s (Figure 3a), incomplete bonding was observed, and the unbonded areas were found along the FPCB pad interface. During ultrasonic bonding, the temperature produced along the bonding interface is not high enough to cause melting of the joint materials. The temperature at the joint during ultrasonic bonding has been reported to be much lower than the melting point of the base metal, and less than 100°C in a Sn-based solder joint (Harman *et al.*, 1977, Kim *et al.*, 2008). Thus, ultrasonic bonding is recognized as a solid state bonding technique (Krzanowski *et al.*, 1990). Although, the temperature at the bonding interface is not enough to cause melting, some heat is produced which contributes to accelerating the diffusion of atoms to form IMC. However, the extent of diffusion is

Figure 2 Schematic diagram of pull test for the bonded joint of FPCB/RPCB

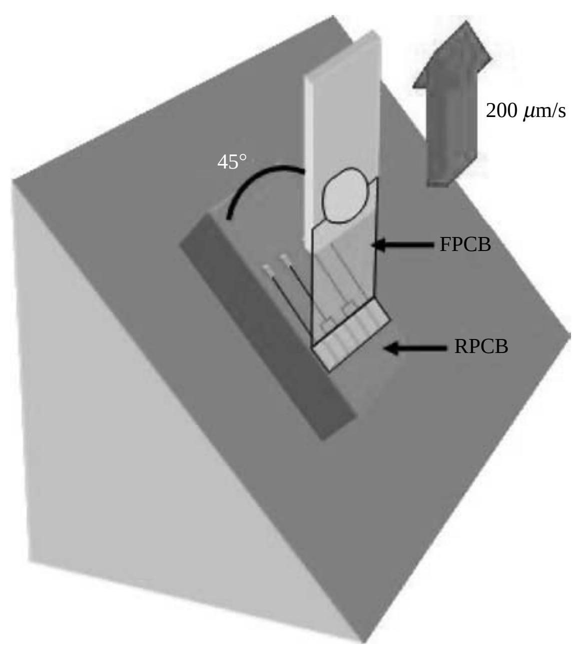

Figure 3 Cross-sections of the bonded joints versus bonding time (US frequency; 20 kHz, power; 1,400 W)

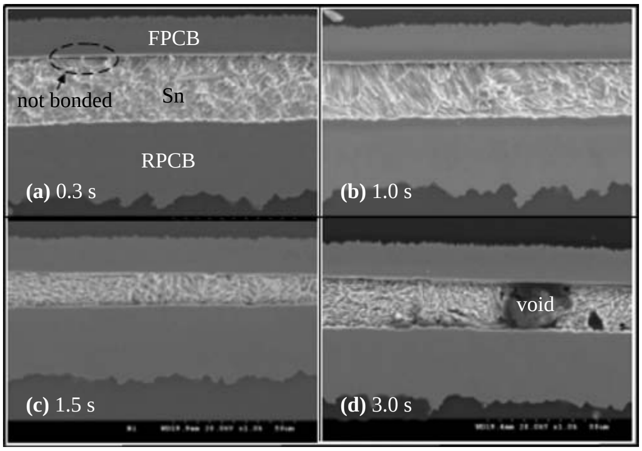

limited due to the short bonding time (Graff *et al.*, 2007). The IMC will be discussed in the following sections.

By increasing bonding time to the range between 0.5 and 1.5 s, the FPCB and RPCB bonded well (see Figures 3(b) and (c)). Especially, the samples of 1.5 s showed an optimum joint free of defects such as unbonded area, voids or cracks. Thus, ultrasonic bonding with longitudinal vibration at ambient temperature between Sn and Au, the surface layers of the pads of FPCB and RPCB, respectively, which had not previously been accomplished (Graff *et al.*, 2007), has now been confirmed to be feasible. Ultrasonic bonding at ambient temperature makes the bonding process and equipment simple. In addition, bonding the pads of FPCB and RPCB directly without ACF can reduce cost, and increase electrical conductivity.

While a parameter range giving good quality bonds was determined, excessive bonding time led to the production of defects. At a bonding time of 3.0 s, voids were formed in the Sn-layer and cracks were observed along the interfacial IMCs of both RPCB and FPCB (see Figure 3(d)). These cracks propagated out to the surface of the joint. The sequence of crack propagation was investigated in detail by bonding samples at intermediate times including 2.0 and 2.5 s. Cross sections from the samples of 2.0, 2.5 and 3.0 s and observed cracking mechanism are illustrated in Figure 4. At 2.0 s voids sized at 15 μm or smaller and micro-cracks were observed. At 2.5 s voids were observed to grow as big as 65 μm length, reaching to the interfaces of both PCBs. With a further increase of bonding time to 3.0 s cracks propagated from the voids along the brittle IMCs. Generally, excessive bonding time during ultrasonic bonding causes accumulation of mechanical fatigue damage in the bonded joint, and it has been reported that in the joint between the Si die and the Au/Cu pads on RPCB with Sn-3.5 percent Ag, excessive bonding time resulted in cracks or voids (Kim *et al.*, 2008).

3.2 Intermetallic compounds in the joints

IMCs produced between the FPCB with Au/Ni/Cu-pad and the Sn-layer were analysed by SEM and EDS. The chemical compositions of IMCs versus ultrasonic bonding time are listed in Table I. In these compositions the Sn content remained almost constant at around 50 atomic percent, and Ni and Cu content changed approximately.

In order to further study the nature of the IMCs, XRD analysis was performed. Figure 5(a) shows the XRD patterns of the IMCs formed on the Sn/FPCB interface. As shown in Figure 5(a), IMCs of Cu_6Sn_5, Ni_3Sn_4, and $Cu_{0.81}Ni_{0.19}$ were confirmed at the interface. These IMCs, except $Cu_{0.81}Ni_{0.19}$, have previously been found in reflow soldered samples (Xu *et al.*, 2005, Yang *et al.*, 2001, Ho *et al.*, 2007). The $Cu_{0.81}Ni_{0.19}$ is known to be produced by mechanical alloying of bimetallic layers from the XRD data file (PDF #47-1406). Since pads of the FPCB were composed of Au/Ni/Cu, mechanical alloying between the Ni and Cu layers could occur during ultrasonic vibration. The Ni_3Sn_4 produced by ultrasound-enhanced diffusion is a frequently observed IMC formed between molten solder and Ni layers during reflow or wave soldering. Meanwhile, the Cu_6Sn_5 between Sn and the Cu layer on the FPCB was also produced, from Cu located under the Ni layer. Although the Cu layer is under the Ni, the thickness of Ni layer was relatively thin at 0.3 μm, and it could be readily disrupted during ultrasonic vibration, resulting in production of Cu_6Sn_5.

Interfacial IMCs formed between the FPCB and the Sn-layer were observed by SEM, and the results as a function of bonding time are given in Figure 6. At 0.3 s IMC was observed along the interface but in irregular patches because of incomplete bonding. At 1.5 s approximately 0.3 μm thickness of interfacial Ni_3Sn_4 was observed, and the thickness did not significantly increase up to 3.0 s of bonding time.

The thickness of Ni_3Sn_4 layers on Ni-pad produced by reflow soldering at around 250°C have been reported as approximately 1-1.5 μm thick (Kim *et al.*, 2003, Lee *et al.*, 2005b). Thus, the Ni_3Sn_4 layer produced by ultrasonic bonding is thinner compared to that of reflow soldering, which is consistent with the lower bonding temperature during ultrasonic bonding. The temperature at the joint during ultrasonic bonding with Sn-based solder has been reported as not higher than 100°C (Kim *et al.*, 2008).

IMCs produced between the RPCB with Cu-pad and Sn-layer were analysed by EDS, and the results are shown in Table II. Cu-contents in the IMCs were almost constant with ultrasonic bonding time, in the range of 46-58 atomic percent, and Sn of 42-54 atomic percent.

Figure 5(b) shows the X-ray diffraction patterns taken from a Sn/Cu-pad on the RPCB interface, where the pad was composed of Sn and Cu layers. As shown in Figure 5(b), IMC of Cu_6Sn_5 was observed, as well as metallic Sn and Cu. This IMC of type Cu_6Sn_5 is a common one found on molten soldered samples on Cu-pads using Sn-based solder (Li *et al.*, 2003, Kwon, 2007). Thus, the initial IMC of Cu_6Sn_5 produced during dipping of RPCB to molten Sn bath was evidently retained after the ultrasonic bonding.

The thickness of Cu_6Sn_5 layers between Sn and the Cu-pad on RPCB versus ultrasonic bonding time was estimated from SEM observations (see Figure 7). At 0.3 s the thickness of IMC was 1.1 μm and it had a scallop shape type like typical Cu_6Sn_5 produced by reflow soldering (Wang *et al.*, 2003). IMC on the RPCB was formed firstly in the molten Sn bath, and thus it is thicker than that on the FPCB at the same bonding time. The Cu_6Sn_5 layer became relatively flat at 1.5 s due to abrasion during ultrasonic vibration. However, the thickness didn't increase significantly with increasing bonding time up to 3.0 s. Ultrasonic vibration and low bonding temperature should act to suppress overgrowth of the IMC.

Soldering & Surface Mount Technology
Volume 21 · Number 1 · 2009 · 4–10

Figure 4 Illustration of cracking mechanisms along the bonded joint

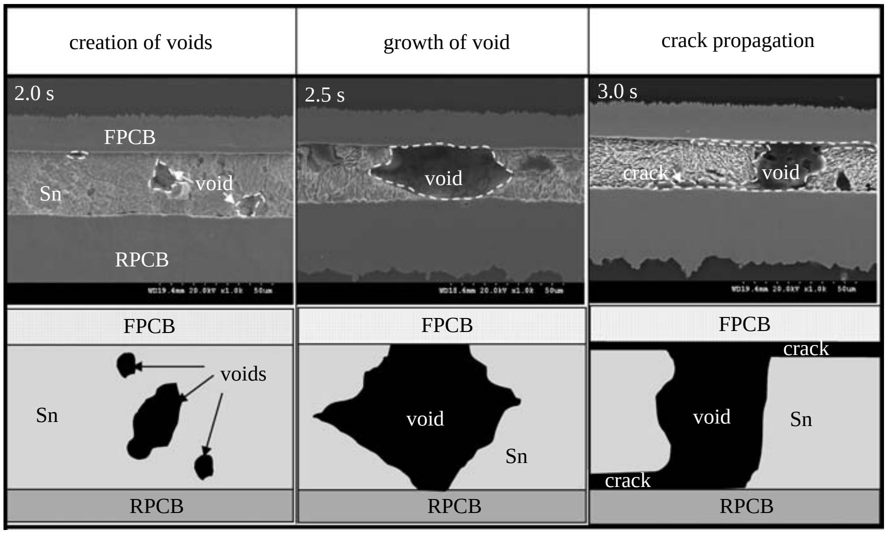

Table I Compositions of IMCs between FPCB and Sn layer by EDS analysis

Bonding time (s)	0.3	1.0	1.5	3.0
Ni atomic percent	25.83	29.78	31.91	12.74
Cu atomic percent	24.06	17.45	15.17	34.65
Sn atomic percent	50.11	52.77	52.92	52.61

3.3 Bond strength

Figure 8 shows the bond strength of the FPCB to RPCB joints versus bonding time. The bond strength increased with bonding time up to 1.5 s, averaging 7.48, 10.68 and 12.48 N for 0.3, 1.0 and 1.5 s, respectively. However, the strength decreased drastically to 5.70 N at 3.0 s, and the reason is believed to be the voids and cracks found at the joint due to excessive bonding time.

In order to understand the ultrasonic bonding phenomena occurring between FPCB and RPCB, the footprints from the fracture surfaces of FPCB pads were examined. For the examination, Sn-content on the FPCB which originated from the coating on the RPCB was analysed by EDS. As shown in Figure 9(a), at 0.3 s Sn was distributed mostly along the edge of the fracture surface, and only a few Sn particles were seen in other areas. With increasing bonding time to 1.0 s, the Sn was more distributed in the centre part of the fracture surface, see Figure 9(b). At the optimum bonding condition of 1.5 s, Sn was found on the whole area of the bond as shown in Figure 9(c).

From this result the bonding process can be understood as follows:

1 At the initial stage of bonding, asperities on the pads of both FPCB and RPCB contact each other through the whole area under bonding pressure.
2 With application of ultrasound, bonding starts from the edge of the pads. In ultrasonic wire bonding, it has previously been suggested that the normal stress on the edges of the contact zone is lower than at the center of the pad, and thus the edge is more easily able to slide and bonding occurs there first (Lum *et al.*, 2006).
3 With increasing bonding time, bonding propagates to the central part of the pad. That is, acoustic weakening or ultrasonic softening occurs along the bonding interfaces with increasing bonding time, which results in gross sliding of the bonding interfaces. Then finally, the centre part of the pad is bonded.

This bonding procedure shows similar behaviour to that of ultrasonic wire bonding studied by the authors (Lum *et al.*, 2006, Lum *et al.*, 2005). In the authors' studies of the ultrasonic bonding process, the bonding proceeded from edge to centre of the joint with ultrasonic power. In this study, a similar phenomenon was found with bonding time.

In future studies, we would like to investigate the effect of Sn-layer thickness, bonding parameters and joint quality such as moisture intake, temperature cycling, high temperature storage and, etc.

4. Conclusions

FPCB with Au/Ni/Cu-pads were directly bonded to RPCB with Sn/Cu-pads by the ultrasonic bonding process at ambient temperature. The results can be summarized as follows:

1 Direct room temperature ultrasonic bonding of contact pad arrays between FPCB and RPCB was performed successfully and robust joints were obtained at 1.5 s bonding time. Ultrasonic bonding of contact pads coated with Sn to other metals was confirmed to be feasible.
2 On the FPCB side of the joints, Cu_6Sn_5 and Ni_3Sn_4 were formed between the Au/Ni/Cu pads and the facing Sn layer, and $Cu_{0.81}Ni_{0.19}$ was produced by mechanical alloying between Ni and Cu layers during ultrasonic vibration. On the RPCB side Cu_6Sn_5 was produced between Cu pads and the Sn coating. Intermetallic compounds produced by ultrasonic bonding at room temperature were similar to those normally resulting from molten soldering, except for $Cu_{0.81}Ni_{0.19}$.
3 Bonding strength between FPCB and RPCB increased with bonding time up to 1.5 s, and the strength with the optimum procedure was 12.47 N. Excessive bonding time

Figure 5 XRD patterns for the IMCs on the bonded interfaces (bonding time 1.5 s): (a) IMCs on FPCB pad; (b) IMC on RPCB pad

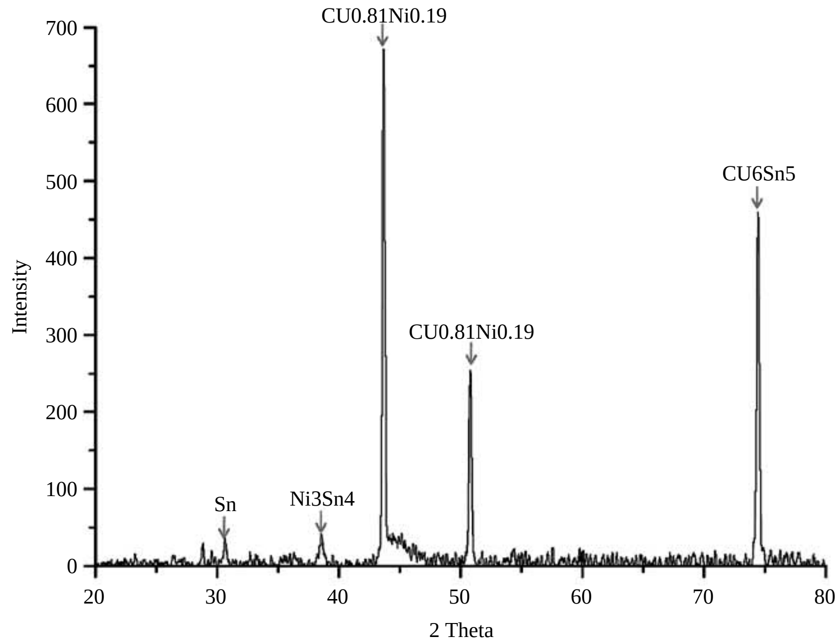

(a)

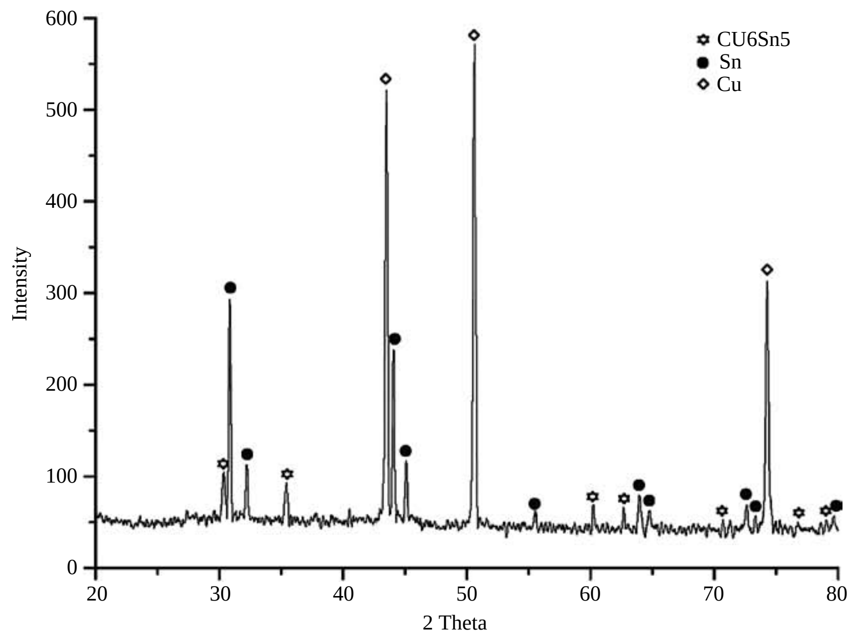

(b)

Figure 6 Bonded interfaces and IMCs between Sn layer and FPCB versus bonding time (US frequency; 20 kHz, power; 1,400 W)

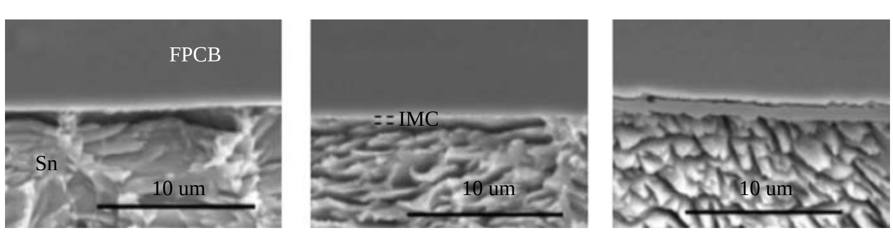

(a) 0.3 s **(b)** 1.5 s **(c)** 3.0 s

Table II Compositions of IMCs between RPCB and Sn layer by EDS analysis

Bonding time (s)	0.3	1.0	1.5	3.0
Cu atomic (percent)	57.95	51.87	45.73	53.78
Sn atomic (percent)	42.05	48.13	54.27	46.22

Figure 7 Bonded interfaces and IMCs between Sn layer and RPCB versus bonding time (US frequency; 20 kHz, power; 1,400 W)

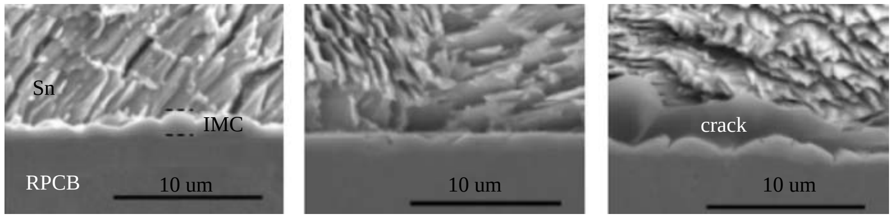

(a) 0.3 s **(b)** 1.5 s **(c)** 3.0 s

Figure 8 Pull strengths of bonded joints between FPCB and RPCB

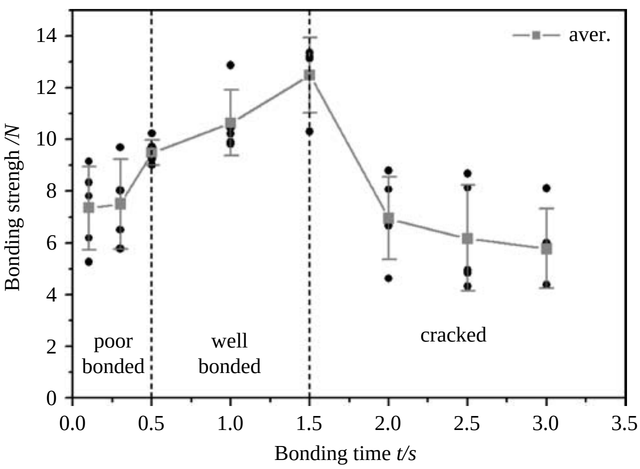

Figure 9 Sn-distributions on the footprints from the fractured surfaces of FPCB pad versus bonding time

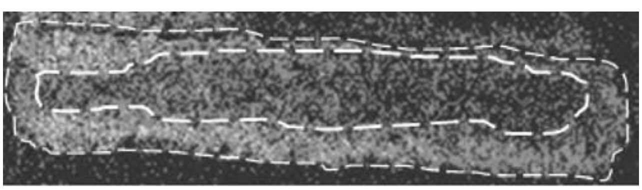

(a) 0.3 sec

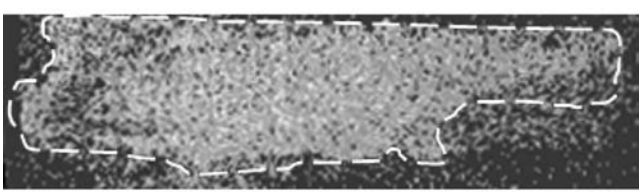

(b) 1.0 sec

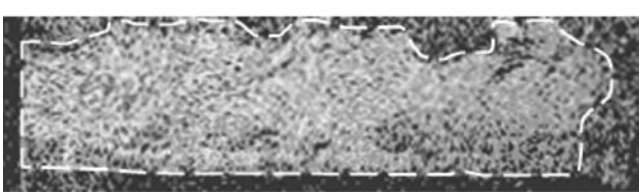

(c) 1.5 sec

such as 3.0 s caused a drastic decrease of strength to 5.75 N due to voids and cracks in the bonded joints.

4. Through the analysis of the footprints from the fractured surfaces of FPCB pads, ultrasonic bonding was found to start from the pad-edge and then expanded to the centre of the pad with increased bonding time.

References

Chan, Y.H., Kim, J.K., Liu, D., Liu, P.C.K., Cheung, Y.M. and Ng, M.W. (2006), "Comparative performance of gold wire bonding on rigid and flexible substrates", *J. Mater. Sci. Mater. Elec.*, Vol. 17 No. 8, pp. 597-606.

Fan, S.H. and Chan, Y.C. (2003), "Current carrying capacity of anisotropic-conductive film joints for the flip chip on flex applications", *J. Elec. Mater.*, Vol. 32 No. 2, pp. 101-8.

Frisk, L. and Kokko, K. (2006), "The effects of chip and substrate thickness on the reliability of ACA bonded flip chip joints", *Sold. and Surf. Mount. Tech.*, Vol. 18 No. 4, pp. 28-37.

Graff, K.F., Devine, J.F., Keltos, J. and Zhou, N.Y. (2007), *Welding Handbook*, Vol. 3 (Amer. Weld. Soc., 9th ed.), Miami, FL, pp. 263-301.

Harman, G.G. and Albers, J. (1977), "The ultrasonic welding mechanism as applied to aluminum- and gold-wire bonding in microelectronics", *IEEE Trans. Parts Hyb. Pack.*, Vol. PHP-13, pp. 406-12.

Ho, C.E., Yang, S.C. and Kao, C.R. (2007), "Interfacial reaction issues for lead-free electronic solders", *J. Mater. Sci.: Mater. Elec.*, pp. 155-74.

Hong, S.M., Kang, C.S. and Jung, J.P. (2002), "Fluxless Sn-3.5mass%Ag solder bump flip chip bonding by ultrasonic wave", *Mater. Trans.*, Vol. 43 No. 6, pp. 1336-40.

Kim, J., Chiao, M. and Lin, L. (2002), "Ultrasonic bonding of In/Au and Al/Al for hermetic sealing of MEMS packaging", *Proceedings IEEE International Conference on Micro Electro Mechanical Systems (MEMS)*, pp. 415-8.

Kim, J.H., Jeong, S.W., Kim, H.D. and Lee, H.M. (2003), "Morphological transition of interfacial Ni3Sn4 grains at the Sn-3.5Ag/Ni joint", *J. Elec. Mater.*, Vol. 32 No. 11, pp. 1228-34.

Kim, J.M., Jung, J.P., Zhou, Y.N. and Kim, J.Y. (2008), "Ambient temperature ultrasonic bonding of Si-dice using Sn-3.5 wt%Ag", *J. Elect. Mater.*, Vol. 37 No. 3, pp. 324-30.

Krzanowski, J.E. (1990), "A transmission electron microscopy study of ultrasonic wire bonding", *IEEE Trans. Compo. Hyb. Manu. Tech.*, Vol. 13 No. 1, pp. 176-81.

Kwon, D. *et al.* (2007), *A Guide to Lead-free Solders – Physical Metallurgy and Reliability*, Springer, London, pp. 97-126.

Lee, J., Kim, J.H. and Yoo, C.D. (2005a), "Thermosonic bonding of lead-free solder with metal bump for flip-chip bonding", *J. Elect. Mater.*, Vol. 34 No. 1, pp. 96-102.

Lee, J.W., Lee, Z.H. and Lee, H.M. *et al.* (2005b), "Formation of intermetallic compounds in the ni bearing lead free composite solders", *Mater. Trans.*, Vol. 46 No. 11, pp. 2344-50.

Lee, J.B., Koo, J.M., Hong, S.M., Shin, H., Moon, Y.J., Jung, J.M., Yoo, C.D. and Jung, S.B. (2008), "Longitudinal ultrasonic bonding of electrodes between rigid and flexible printed circuit boards", *Jpn. J. App. Phy.*, Vol. 475, pp. 4300-4.

Li, G.Y. and Chen, B.L. (2003), "Formation and growth kinetics of interfacial intermetallics in Pb-free solder joint", *IEEE Trans. Compo. Pack. Tech.*, Vol. 26 No. 3, pp. 651-8.

Lum, I., Jung, J.P. and Zhou, Y. (2005), "Bonding mechanism in ultrasonic gold ball bonds on copper substrate", *Metall. and Mater. Trans. A.*, Vol. 36A No. 5, pp. 1279-1286A.

Lum, I., Mayer, M. and Zhou, Y. (2006), "Footprint study of ultrasonic wedge-bonding with aluminium wire on copper substrate", *J. Elec. Mater.*, Vol. 35 No. 3, pp. 433-42.

Seppala, A., Aalto, K. and Ristolainen, E. (2003), "Reducing bonding cycle time of adhesive flip chip Process", *Sold. and Surf. Mount. Tech.*, Vol. 15 No. 1, pp. 16-20.

Shi, W. and Little, T. (2000), "Mechanisms of ultrasonic joining of textile materials", *Int'l J. Clothing Sci. Tech.*, Vol. 12 No. 5, pp. 331-50.

Wang, S.J. and Liu, C.Y. (2003), "Study of interaction between Cu-Sn and Ni-Sn interfacial reactions by Ni-Sn3.5Ag-Cu sandwich structures", *J. Elec. Mater.*, Vol. 32 No. 11, pp. 1303-9.

Wu, C.M.A., Liu, J. and Yeung, N.H. (2001), "The effect of bump heights on the reliability of ACF in flip-chip", *Sold. and Surf. Mount. Tech.*, Vol. 13 No. 1, pp. 25-30.

Xu, L., Pang, J.H.L. and Che, F.X. (2005), "Intermetallic growth and failure study for Sn-Ag-Cu/ENIG PBGA solder joints subject to thermal cycling", IEEE Electronic Compo. Tech. Conf., pp. 682-6.

Yang, S.T., Chung, Y. and Kim, Y.H. (2001), "Intermetallic growth between Sn-Ag-(Cu) solder and Ni", IEEE Electronic Mater. Pack. Conf., pp. 219-24.

Further reading

The International Centre for Diffraction Data (n.d.), PDF(Powder Diffraction File) #47-1406.

Corresponding author

Jae-Pil Jung can be contacted at: jpjung@uos.ac.kr